Regulatory Peptides 181 (2013) 37–44

Contents lists available at SciVerse ScienceDirect

Regulatory Peptides

journal homepage: www.elsevier.com/locate/regpep

Binding affinities and activation of Asp712Ala and Cys100Ser mutated kinin B_1 receptor forms suggest a bimodal scheme for the molecule of bound-DABK

E.S. Rodrigues [1], R.P. Martin [1], R.F. Silva [1], C.R. Nakaie [1], L. Oliveira [1], S.I. Shimuta *

Biophysics Department, Universidade Federal de São Paulo, Rua Botucatu, 862 7th floor, São Paulo, SP, Brazil

ARTICLE INFO

Article history:
Received 31 July 2012
Received in revised form 30 November 2012
Accepted 17 December 2012
Available online 11 January 2013

Keywords:
DesArg9BK
Kinin B1 receptor
Angiotensin II type I receptor

ABSTRACT

Mutant forms of kinin B_1 receptor (B_1R) and analogs of the full agonist des-Arg^9-bradykinin (DABK) were investigated aiming to verify the importance of selected receptor residues and of each agonist-peptide residue in the specific binding and activation. Linked by a specific disulfide bond (Cys^{100}–Cys^{650}), the N-terminal (N_t) and the EC3 loop C-terminal (C_t) segments of angiotensin II (AngII) receptor 1 (AT_1R) have been identified to form an extracellular site for binding the agonist N_t segment (Asp^1 and Arg^2 residues). Asp^{712} residue at the receptor EC3 loop binds the peptide Arg^2 residue. By homology, a similar site might be considered for DABK binding to B_1R since this receptor contains the same structural elements for composing the site in AT_1R, namely the disulfide bond and the EC3 loop Asp^{712} residue. DABK, Ala^n-DABK analogs (n = Ala^1-, Ala^2-, Ala^3-, Ala^4-, Ala^5-, Ala^6-, Ala^7-, Ala^8-DABK), and other analogs were selected to binding wild-type, Asp712Ala and Cys100Ser mutated B_1R receptors. The results obtained suggested that the same bimodal scheme adopted for AngII-AT_1R system may be applied to DABK binding to B_1R. The most crucial similarity in the two cases is that the N_t segments of peptides equally bind to the homologous Asp^{712} residue of both AT_1R and B_1R extracellular sites. Confirming this preliminary supposition, mutation of residues located at the B_1R extracellular site as EC3 loop Asp^{712} and Cys^{100} caused the same modifications in biological assays observed in AT_1R submitted to homologous mutations, such as significant weakening of agonist binding and reduction of post-receptor-activation processes. These findings provided enough support for defining a site that determines the specific binding of DABK to B_1R receptors.

1. Introduction

Des-Arg^9-bradykinin (DABK)[2] is the regular agonist of kinin B_1 receptor (B_1R), a member of family A G-protein-coupled receptors (AGPCRs) [1]. As the structure of all these receptors, B_1R consists of a seven transmembrane-helix bundle (7TM), linked to extracellular N-terminal (N_t) and cytosolic C-terminal (C_t) segments, with the seven helices alternately connected by three extracellular (EC) and three cytosolic (IC) loops [2].

At the present time, as most of the AGPCR sequences are known, a conserved motif has been recognized in all types of angiotensin II (AngII), bradykinin (BK), endothelin, chemokine, purine and Cys-leukotriene receptors and some types of neuropeptide receptors, consisting of an insertion of 8–10 residues in the middle of EC3 loop, including a conserved residue of Cys^{650} supposedly making a disulfide bond with a second conserved Cys^{100} residue located at the N_t segment (Figs. 1 and 2), [3]. This pattern was then investigated for function, especially in AT_1R receptors, thus revealing that the AngII N-terminal segment (Asp^1 and Arg^2 residues) binds to receptor EC3 loop and N_t segment residues [4–8] leading the conserved motif to be classified as an extracellular sub-site for agonist binding [9].

Regarding B_1R receptors, binding patterns of DABK seem to be similar to those observed in AngII interaction with AT_1R. (1) The agonist C_t carboxylate group is stabilized by electrostatic contacts with helix III Lys^{323} [10] and helix V Arg^{508} [11] both at the external half of the receptor 7TM central cavity. (2) The residues in the external segment of the kinin receptors' helix VI appear to be linked to high-affinity binding [10]. (3) The agonist N-terminal R^1 residue binds to receptor residues located at the other side of the 7TM structure as EC3 loop Asp^{712} (and Glu^{709}) [12]. The homology of binding between B_1R and AT_1R is assumed because Asp^{712} residue of the former receptor corresponds to the Asp^{712} residue of AT_1R extracellular site at which the AngII Arg^2 residue is supposed to bind [6].

In the current work, B_1R and DABK or analogs are studied aiming to ascertain the importance of some receptor residues and each agonist residue for specific binding, production of IP_3 or increase of the cytosolic calcium levels. Particularly, effects due to modifications of the B_1R extracellular site were monitored by analyzing the binding dependence on the N_t Arg^1 residue of DABK. Studies with this approach have been previously carried out with AT_1R leading to the discovery that

* Corresponding author. Tel.: +55 11 55724583.
E-mail address: sshimuta@unifesp.br (S.I. Shimuta).
[1] Tel.: +55 11 55724583.
[2] One- and three-letter codes for peptide and protein positions, respectively; numbering system for AGPCR positions in Fig. 2 and GPCRDB [1].

0167-0115
http://dx.doi.org/10.1016/j.regpep.2012.12.014

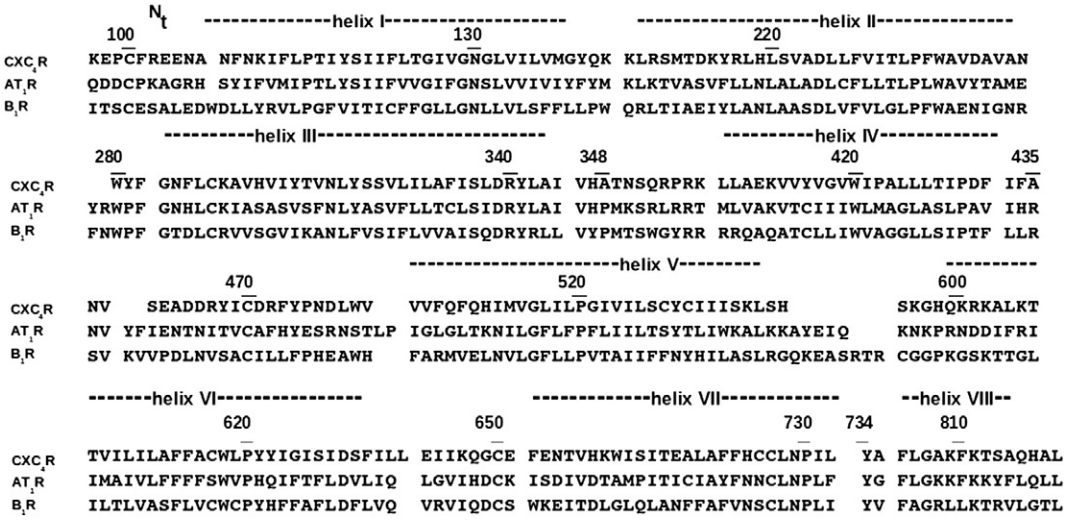

Fig. 1. Alignment of angiotensin II type I (AT_1R), kinin B_1 (B_1R) and chemokine (CXC_4R) receptors. The residue positions were numbered according to GPCRDB system. Segments of sequences belonging to a same secondary structure (alpha-helix or beta structure) have a referential 3-digit number: the first digit designates the number of helix (1–8 for helices I–VIII) and other intermediate secondary structures; the second and third digits form a number that defines a certain position in the respective segment. Thus, different positions are numbered according to the segments at which they are located and the distance from the respective referentials.

mutation to Ala of two residues, EC3 loop Asp^{712} and Cys^{100} (or Cys^{650}) abolishes the Arg^2-dependent binding of AngII to the receptor extracellular site [3,7]. As AngII, DABK also displays an Arg residue at its N_t segment and thus it might be postulated that B_1R extracellular site could play the same role observed with AT_1R, upon binding its specific agonist. Herein this possibility was confirmed from experimental results obtained by binding DABK and analogs to Asp712Ala and Cys100Ser mutants' forms of B_1R.

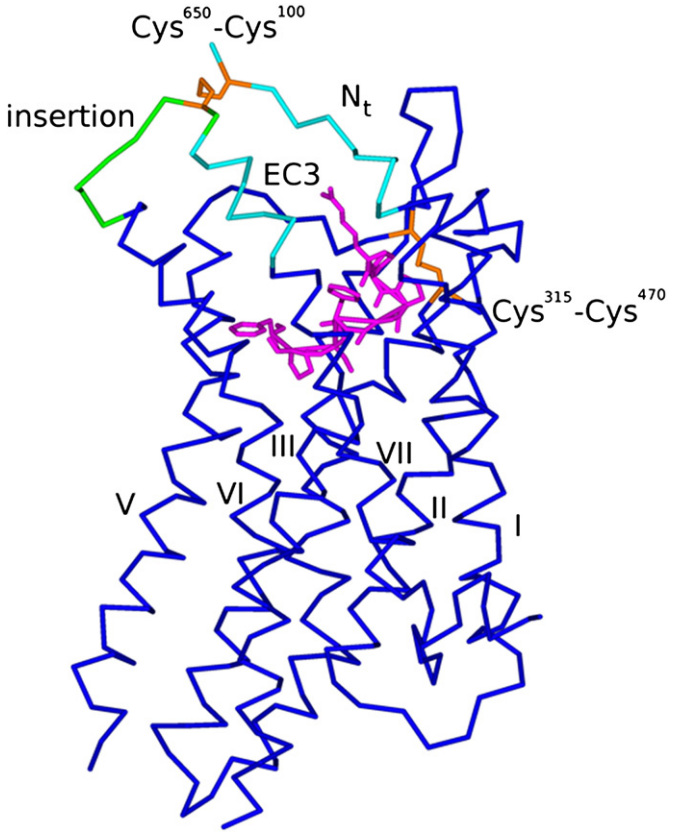

Fig. 2. Structure of G-protein-coupled receptors with seven transmembrane-helix bundle. Overview of the structure showing the receptor seven transmembrane-helix bundle in dark blue (only helix IV is not identified) and the very conserved Cys^{315}–Cys^{470} disulfide bond in gold. The receptor extracellular site is shown in the top of the figure consisting of N-terminal and EC3 segments (light blue), the Cys^{650}–Cys^{100} disulfide bond (gold) and the residue insertion (green). The peptide inserted into a postulated binding site is shown in magenta.)

2. Material and methods

2.1. Peptides synthesis

The peptides were synthesized manually in accordance with the standard tert-butyloxycarbonil (Boc) protocol [13,14]. In the Boc chemistry, after coupling the C_t amino acid to the resin, the successive α-amino group deprotection and neutralization steps were performed in 30% TFA (trifluoroacetic acid)/DCM (dichloromethane) (30 min) and 10% TEA (triethylamine)/DCM (10 min). The amino acids were coupled with 3-fold excess, using DIC (N,N′-diisopropylcarbodiimide)/HOBt (1-hydroxybenzotriazole) in DMF (N,N-dimethylformamide). After a 3 h coupling period, the qualitative ninhydrin test was performed to estimate the completeness of the reaction. To check the purity of the synthesized peptide sequence attached to the resin, cleavage reactions with small aliquots of resin were carried out in anhydrous HF, at 0 °C for 2 h. Analytical HPLC (High performance liquid chromatography), as well as LC/ESI-M (Liquid chromatography/Electrospray ionization -mass spectrometry) and amino acid analysis were used to check the homogeneity of each synthesized resin-bound peptide sequence. The synthesized analogs are presented in Table 1.

2.2. Biological activities of the peptides

Experiments were carried out with C57BL/6J mice from the Centro de Desenvolvimento de Modelos Experimentais da Universidade Federal de São Paulo (CEDEME-UNIFESP). The animals were maintained on standard mouse chow at 21–23 °C and kept on 12 h light:12 h dark cycle and allowed ad libitum access to food and water. After 12–16 weeks, old mice weighing 26–30 g were sacrificed by cervical dislocation and exsanguination. This study was in accordance with current guidelines for the care of laboratory animals and ethical guidelines for investigations approved by the Animal Care Committee of UNIFESP.

All experiments to assess the biological activities of the new peptides were performed in the mouse stomach, which contains functional B_2 and B_1 receptors. The stomach fundus isolated from mouse has been reported to respond to the agonists BK and DABK [15,16]

Table 1
The natural agonist is the des-Arg^9-BK (DABK) (compound 2); DABK analogs (1 and 3–12).

Compound	Analog	Sequence							
1	DABK		R^1	P^2	P^3	G^4	F^5	S^6	P^7	F^8
2	A^1-DABK		A^1	P^2	P^3	G^4	F^5	S^6	P^7	F^8
3	A^2-DABK		R^1	A^2	P^3	G^4	F^5	S^6	P^7	F^8
4	A^3-DABK		R^1	P^2	A^3	G^4	F^5	S^6	P^7	F^8
5	A^4-DABK		R^1	P^2	P^3	A^4	F^5	S^6	P^7	F^8
6	A^5-DABK		R^1	P^2	P^3	G^4	A^5	S^6	P^7	F^8
7	A^6-DABK		R^1	P^2	P^3	G^4	F^5	A^6	P^7	F^8
8	A^7-DABK		R^1	P^2	P^3	G^4	F^5	S^6	A^7	F^8
9	A^8-DABK		R^1	P^2	P^3	G^4	F^5	S^6	P^7	A^8
10	K^0-DABK	K^0	R^1	P^2	P^3	G^4	F^5	S^6	P^7	F^8
11	K^1-DABK		K^1	P^2	P^3	G^4	F^5	S^6	P^7	F^8
12	L^4-DABK		R^1	P^2	P^3	L^4	F^5	S^6	P^7	F^8

Peptide amino acids are expressed by the one-letter code. A=alanine, R=arginine, P=proline, G=glycine, F=phenylalanine, S=serine, K=lysine.

and quantitative RT-PCR analysis of B_1 and B_2 mRNA expression was described by [17] in this tissue.

Stomach fundus was isolated from mouse, divided in two strips of the longitudinal muscle and mounted into a 5 ml organ baths (Panlab s.l., Cornella, CA, Spain), containing modified Krebs-Ringer solution: 144 mM NaCl, 5 mM KCl, 1.1 mM $MgSO_4$, 25 mM $NaHCO_3$, 1.1 mM NaH_2PO_4, 1.25 mM CaCl and 5.5 mM glucose at 37 °C (pH 7.4) continuously carboxygenated (95% O_2/5% CO_2). Contractile responses to the stimulations with DABK and its analogs were recorded. The resting tension was maintained at 0.5 g and the tissues were left to equilibrate for 90 min, with frequent changing of fresh bathing solution. Following, changes in tension produced by the stimulants were measured with a tension transducer TRI201 (Panlab s.l., Cornella, CA, Spain), through an amplifier Powerlab 4/30 and software Labchart Pro V7 (ADInstruments, Colorado Springs, CO, USA).

Cumulative concentration-contractile response curves were constructed for DABK and analogs, by applying increasing concentrations (0.1 nM to 1 μM) of each agonist to determine the apparent affinity of agonists in terms of pD_2 (the negative logarithm of the concentration of agonist that produces 50% of the maximal effect, EC_{50}) and the maximal effect (E_{max}) was calculated in relation to the effect of 140 mM KCl, which was considered 100%. The curve-fitting analysis for dose-response curves was performed using the GraphPad-Prism 3.0 Program (GraphPad Software, San Diego, CA, US).

2.2.1. Construction of kinin B_1R mutants

The vector pEYFP-N_1B_1R (Clontech Laboratories, Mountain View, CA, US) expressing rat B_1R was gently donated by Santos et al. [11] and used as a template for the mutant Asp712Ala, replacing the Asp^{712} with Ala and Cys100Ser, replacing the Cys^{100} with Ser. The site-directed mutagenesis was performed with QuickChange site-directed mutagenesis kit (Stratagene, Santa Clara, CA, US) according to the manufacturer's instructions. The mutagenesis oligonucleotides used are listed below. For a single Asp712Ala mutant (sense, 5′-GAAGGAGATCACAGCCCTGGGCC TGCAGC-3′ and antisense, 5′-GCTGCAGGCCCAGGGCTGTGATCTCCTTC-3′). Cys100Ser mutant (sense, 5′-GCCAACATTACCTCCAGCGAGAGTGC CCTA-3′ and antisense, 5′-TAGGGCACTCTCGCTGGAGGTAATGTTGGC-3′). All receptor constructs were initially identified by the presence of a diagnostic restriction site and subsequently verified by sequencing.

2.3. Cell culture and transfection

Chinese hamster ovary (CHO) cells were cultured in Dulbecco's modified Eagle's medium — DMEM (Invitrogen, Carlsbad, CA, US) supplemented with 10% of fetal bovine serum, 100 U/ml penicillin, 100 μg/ml streptomycin and 2 mM glutamine (all from Invitrogen, Carlsbad, CA, US). Cultures were maintained at 37 °C in a humidified 5% CO_2 atm. Expression plasmids containing wild-type receptor and B_1R mutated receptors, Asp712Ala and Cys100Ser, were permanently transfected into CHO cells by lipofectamine 2000 (Invitrogen, Carlsbad, CA, US), method according to the manufacturer's instructions and 2 μg of plasmid DNA for each sample. For the establishment of stable cell lines, transfected cultures were maintained in culture medium supplemented with 750 μg of G-418 (Invitrogen, Carlsbad, CA, US).

2.4. Expression of kinin B_1R and mutants in transfected CHO cells

Clones with high expression levels of wild-type B_1R mRNA and of mutated receptors were selected by real-time PCR. CHO cells transfected with the wild-type receptor and mutants were seeded at 1×10^6 cells per well in 6-well plates and left for 24 h at 37 °C. The culture medium was siphoned off and the total RNA was isolated using TRIzol® reagent (Invitrogen, Carlsbad, CA, US), according to the manufacturer's instructions. After purification, the presence of intact RNA was verified on an ethidium bromide-stained agarose gel and the total RNA was submitted to reverse transcription using SuperScript™ III First-Strand reverse transcriptase kit (Invitrogen, Carlsbad, CA, US). To determine the expression of B_1R, real-time PCR was performed with 5 μl of 1:10 dilution cDNA samples pre-obtained, where each reaction was carried out using Taqman Universal PCR Master Mix (Applied Biosystems, Foster City, CA, US), according to the manufacturer's instructions. Primers used for real-time PCR were as follows: murine β-actin (GenBank accession no. NM007393), forward primer 5′-CTGG CCTCACTGTCCACCTT-3′ and reverse primer 5′-CGGACTCATCGTACTC CTGCTT-3′; and probe. 5′-6FAM-CTGATCCACATCTGCT-TAMRA-3′ and rat B_1R (GenBank accession no. NM030851), reverse primer 5′-CAA ACAGGTTGGCCTTGATGAC-3′, forward primer 5′-CTGGCCCTTCGGAAC TGA-3′ and probe 5′-6FAM-CCCGCTGACCACCC-TAMRA-3′.

The real-time PCRs were performed with an ABI PRISM® 7000 sequence detection system (Applied Biosystems, Foster City, CA, US) and cycle conditions were: 50 °C for 2 min, 95 °C for 10 min, followed by 50 cycles of 95 °C for 15 s (melting step), 60 °C for 1 min (anneal/extend step). Increases in the amount of reporter dye fluorescence during the 50 amplification cycles were monitored using Sequence Detector software (SDS version 1.6, Applied Biosystems, Foster City, CA, US). Quantification of the target amount was performed by measuring the threshold cycle, C_T, which is defined as the fractional cycle number at which the fluorescence encounters a fixed threshold. A normalized value to evaluate the mRNA expression was calculated as the difference in the threshold cycle: the C_T values of receptor minus C_T of internal standard (β-actin), resulting in ΔC_T. Since it is uncommon to use ΔC_T parameter as a relative expression parameter due to this logarithmic characteristic, the $2^{-\Delta CT}$ parameter was used to express the relative gene expression data [18]. B_1R mRNA abundance was quantified as a relative value compared with an internal reference, β-actin, of which the abundance was assumed not to change between the varying experimental conditions.

2.5. Heterologous competition binding assay

The transfected CHO cells were seeded at 5×10^4 cells per well in 96-well plates and left for 24 h at 37 °C. The culture medium was siphoned off and the cells were washed twice with wash buffer (mM — Tris–HCl 25, $MgCl_2$ 5, 0.1% BSA, pH 7.4). Then, they were suspended in binding buffer (mM — 25 Tris–HCl, 5 $MgCl_2$, 0.1% BSA and 100 μg/ml bacitracin, pH 7.4) in the presence of a fixed concentration of the radioligand. 5×10^4 cpm/well of des-Arg^{10}[3,4-prolyl-3,4-^{3}H(N)], (62 Ci/mmol) and different concentrations of the unlabelled ligands (DABK and analogs, shown in Table 1) for competition binding assays. The plates were incubated overnight at 4 °C. The binding buffer was siphoned off and the cells were washed twice with cold wash buffer and then lysed with lysis buffer (0.5% SDS and 0.1 mol/l NaOH). Receptor-bound radiolabels were counted to determine inhibition

constant (IC_{50}) values in a MicroBeta^2 plate counter (Perkin-Elmer, Waltham, MA, US). The binding affinity of ligands for BKR_1R and mutants was estimated from inhibition constant (IC_{50}) values obtained from a nonlinear regression analysis of binding curves of GraphPad 3.0 Program (GraphPad Software, San Diego, CA, US).

2.6. IP_3 assay

IP_3 production was determined in the transfected CHO cells to test the functional expression of the wild-type and mutant receptors using HitHunter Inositol (1,4,5)-trisphosphate [IP_3] Assay kit (PerkinElmer, Waltham, MA, US). The cells were harvested and resuspended in PBS without $CaCl_2$ and $MgCl_2$ (mM — KCl 2.7, KH_2PO_4 1.5, NaCl 137 and Na_2HPO_4 8) in a concentration of 50,000 cells per μl. In a 96-well black plate (Perkin-Elmer, Waltham, MA, US), 20 μl of cells per well was added. Then, those cells were stimulated for 20 s with 10 μl of increasing concentration of DABK and analogs (0.1 nM to 1 μM) and quenched with 10 μl perchloric acid 0.2 N (water diluted). The Tracer-Green and Binding Protein (available in the kit) were incubated in a final volume of 20 μl and 40 μl respectively for 5 min in a plate shaker for each. A standard curve was obtained with increasing amounts of IP_3 (6.7×10^{-11} to 1.33×10^{-6} M — available in the kit) under the same protocol described above. The DABK (100 nM) induced effect was tested in the presence and absence of 1 μM R-715, a specific antagonist of B_1R, pre-incubated for 30 min. The fluorescence polarization was detected by Victor X5 microplate reader (Perkin-Elmer, Waltham, MA, US). The data were acquired in triplicate to draw the dose-response curves using the GraphPad 3.0 Program (GraphPad Software, San Diego, CA, US).

2.7. Calcium assay

The transfected CHO cells expressing the B_1R and the mutants were seeded at 5×10^5 cells per well in a 96-well black microplate with clean bottom (Nunc, Rochester, NY, US) and left for 24 h at 37 °C. The cells were washed with HBSS, pH 7.4 (mM — $CaCl_2$ 1.26, $MgCl_2$–$6H_2O$ 0.5, $MgSO_4$–$7H_2O$ 0.4, KCl 5.3, KH_2PO_4 0.4, $NaHCO_3$ 4.1, NaCl 138, Na_2HPO_4 0.3, D-glucose 5.5, HEPES 20), and thereafter incubated with 100 μl of Fluo-4 non-wash with 2.5 mM of probenecid for 30–45 min in the dark at 37 °C. The fluorescence signal was read in the Victor X5 microplate reader (Perkin-Elmer, Waltham, MA, US), and the values obtained from non-stimulated cells were considered to be the basal Ca^{2+} level and those obtained from cells stimulated with increasing concentrations of DABK or analogs (0.1 nM to 1 μM) were considered as the variations in the $[Ca^{2+}]_i$ levels. The calcium measurements were performed using Fluo4 NW Calcium Assay kit (Molecular Probes, Eugene, OR, US).

One dose of the peptide was added into each well and the results were used to draw the sigmoidal dose-response curve. At the end of each experiment 1 μM ionomycin (a Ca^{2+} ionophore) was administered to expose the cytosolic Fluo-4NW to the free extracellular Ca^{2+} to get the maximal fluorescence signal (added F_{max}) and 5 mM of EGTA (ethylene glycol tetraacetic acid) was to chelate all free Ca^{2+} in order to get the minimum signal, equivalent to the cell autofluorescence value (F_{min}).

The Ca^{2+} intracellular concentration $[Ca^{2+}]_i$ was calculated using the following formula (Grynkiewicz et al., 1985).

$$\left[Ca^{2+}\right]_i = K_d \times \left(\frac{F-F_{min}}{F_{max}-F}\right)$$

where,

Kd dissociation constant of Fluo-3 equals 450

F the fluorescence signal obtained with 496 nm excitation and 525 nm emission.

F_{min} the fluorescence signal obtained in the EGTA presence (5 mM).

F_{max} the fluorescence signal obtained in the presence of ionomycin (1 μM).

2.8. Modeling procedure for angiotensin and kinin receptors

Based on sequence alignments of Fig. 1, angiotensin II type I and kinin B_1 receptors were built by homology via the WHAT IF program [19], to the CXCR4 receptor, the first AGPCR possessing sequence features resembling the extracellular site, for which a high-resolution 3D structure has been determined [20].

2.9. Statistical analysis

All data are shown as mean ± S.D. (n), number of experiments. Statistical analyses were performed using two-way ANOVA followed by post-test Bonferroni. For statistical comparison, 95% confidence intervals were used.

3. Results

3.1. Biological activity of DABK and analogs

The biological activity of DABK and analogs mediated by B_1R (Table 1) was measured by parameters of apparent affinity (pD_2) and E_{max} (Table 2) through mechanical recordings of the contractile responses of stomach fundus isolated from mouse. Affinity was kept at wild-agonist level by A^6-DABK (compound 7); it was slightly increased for K^1-DABK (compound 11); it was slightly reduced for A^7-DABK (compound 8) and K^0-DABK (compound 10); it was reduced for A^2-, A^3-, A^4-, A^5- and A^8-DABK (in order. compounds 3, 4, 5, 6 and 9) and very reduced for A^1-, L^4-DABK (compounds 2 and 12). Thus, the crucial positions for binding of DABK were R^1, P^2, P^3, G^4, F^5 and F^8 being S^6 and P^7 less important. Lys side-chain at the position 1 can replace Arg; Lys added at the position 0 reduced the binding. At the position 4, the presence of any residue instead of Gly is deleterious for binding. E_{max} values produced by different analogs of DABK varied from 27% to 97% whereas that value for the control DABK was 59% (Table 2).

Table 2
Apparent affinity and maximal effect induced by DABK and analogs on mice stomach fundus.

Compound	Analogs	pD_2	E_{max} (% KCl)
1	DABK	8.1 ± 0.3 (7)	59 ± 6 (7)
2	A^1-DABK	ND	ND
3	A^2-DABK	7.0 ± 0.3 (5)[a]	27 ± 2 (5)[a]
4	A^3-DABK	7.1 ± 0.3 (4)[a]	42 ± 4 (4)[a]
5	A^4-DABK	7.0 ± 0.1 (3)[a]	53 ± 2 (3)
6	A^5-DABK	7.4 ± 0.3 (3)[a]	55 ± 2 (3)
7	A^6-DABK	8.1 ± 0.2 (6)	51 ± 3 (6)
8	A^7-DABK	8.0 ± 0.3 (3)	52 ± 6 (3)
9	A^8-DABK	7.1 ± 0.3 (3)[a]	30 ± 1 (3)[a]
10	K^0-DABK	7.5 ± 0.3 (4)	57 ± 4 (4)
11	K^1-DABK	8.6 ± 0.2 (4)[a]	97 ± 8 (4)[a]
12	L^4-DABK	ND	ND

DABK and DABK analogs-induced isometric contractile responses in mice stomach fundus. The pD_2 values (negative logarithm of the agonist concentration (M) that induces 50% of the maximal response) were extracted from the concentration-response sigmoid logistic curves. The maximal effect (E_{max}) was calculated in relation to the effect of 140 mM KCl, which was considered 100%. ND, not determined. Data are means ± S.D. and (n) number of experiments.

[a] Different from DABK. $P<0.05$. DABK = Arg^1-Pro^2-Pro^3-Gly^4-Phe^5-Ser^7-Pro^7-Phe^8.

3.2. B_1R and mutant expression in transfected CHO cells

CHO cells were permanently transfected with the plasmid containing the coding region for the wild-type rat B_1R and the coding region for B_1R carrying the proposed mutations and with an empty plasmid (mock cells). The expression of the B_1R gene in these cells was evaluated by real-time PCR, by radioligand binding studies and by a functional assay on the IP_3 production and changes in intracellular calcium concentration in response to B_1R agonist, DABK (Fig. 3). Fig. 3A shows the mRNA expression of cell clones expressing the B_1R and mutants selected, with high and comparable levels between them. In the binding study, cells expressing only the B_1R receptor or B_1R mutants were able to bind specifically the B_1R agonist with high affinity, whereas mock cells displayed no binding for the agonist (Fig. 3B). Furthermore, DABK was able to elicit a concentration-response effect on the IP3 production in CHO cells expressing the B_1R or mutant receptor but not in mock cells (Fig. 3C). This effect was inhibited by the specific B_1R antagonist R-715, showing the expression of a functional membrane receptor (Fig. 3D).

Table 3
Binding affinity of DABK and analogs for wild-type and mutant kinin B_1 receptor.

Compound	Analogs	WT	Asp712Ala	Cys100Ser
		IC_{50} (nM)		
1	DABK	3.1 ± 1.6 (3)	370.5 ± 1.1 (3)[b]	93.2 ± 1.1 (3)[b]
2	A^1-DABK	152 ± 0.6 (3)[a]	171.9 ± 1.1 (3)[b]	108.1 ± 0.1 (3)[b]
3	A^2-DABK	61.5 ± 1.4 (3)[a]	417 ± 1.1 (3)[b]	143.2 ± 1.3 (3)[b]
4	A^3-DABK	45.9 ± 1.1 (3)[a]	507.6 ± 1.0 (3)[b]	193.5 ± 1.4 (3)[b]
5	A^4-DABK	56.4 ± 1.1 (3)[a]	639.6 ± 1.0 (3)[b]	220.6 ± 1.1 (3)[b]
6	A^5-DABK	6.8 ± 1.2 (3)[a]	384 ± 1.2 (3)[b]	101.3 ± 1.3 (3)[b]
7	A^6-DABK	2.3 ± 1.1 (3)	216.2 ± 1.0 (3)[b]	78.9 ± 1.3 (3)[b]
8	A^7-DABK	7.8 ± 1.2 (3)[a]	144.9 ± 1.1 (3)[b]	45.9 ± 1.1 (3)[b]
9	A^8-DABK	64.6 ± 1.1 (3)[a]	797.4 ± 1.0 (3)[b]	367.8 ± 1.1 (3)[b]
10	K^0-DABK	23.8 ± 1.3 (3)[a]	133.3 ± 1.1 (3)[b]	74.6 ± 1.2 (3)[b]
11	K^1-DABK	3.2 ± 1.4 (3)	387.6 ± 1.5 (3)[b]	55.4 ± 1.4 (3)[b]
12	L^4-DABK	84.8 ± 1.6 (3)[a]	943.9 ± 1.7 (3)[b]	109.4 ± 1.5 (3)[b]

Competition binding affinity was performed using des-Arg^{10}[3,4-prolyl-3,4-^{3}H(N)] and increasing concentrations of the unlabeled DABK and DABK analogs in cells expressing WT and kinin B_1 receptor mutants. Data are means ± S.D. and (n) number of experiments. DABK = Arg^1-Pro^2-Pro^3-Gly^4-Phe^5-Ser^7-Pro^7-Phe^8.
[a] Different from DABK. $P<0.05$.
[b] Different from respective peptide from WT receptor. $P<0.05$.

3.2.1. Parameters for interaction between B_1R and DABK or analogs

Data from binding assays, the IC_{50} value for binding affinity of DABK analogs to B_1R was about 3 nM (Table 3), whereas EC_{50} for production of IP_3 and increase of cytoplasmic calcium was 6 and 4 nM (Tables 4 and 5) respectively. The dependence of IC_{50} values for binding affinity, EC_{50} for IP_3 formation and increase of intracellular calcium, on the modified residues of DABK followed the same pattern observed with biological activity results (Table 2). Also in agreement with biological activity results, E_{max} values for the three analyses were little impaired being rather independent of residue modifications.

The crucial positions for DABK binding were R^1, P^2, P^3, and G^4 at the N_t side segment and at the C_t F^8, whereas the intermediate 5–7 positions were less important (Tables 3–5). For instance, the affinity binding of DABK analogs with Ala at the positions 1–4 and 8 was low with IC_{50} values varying from 50 to 150 nM, whereas those analogs with A^5-, A^6- and A^7-DABK had stronger binding with IC_{50} values

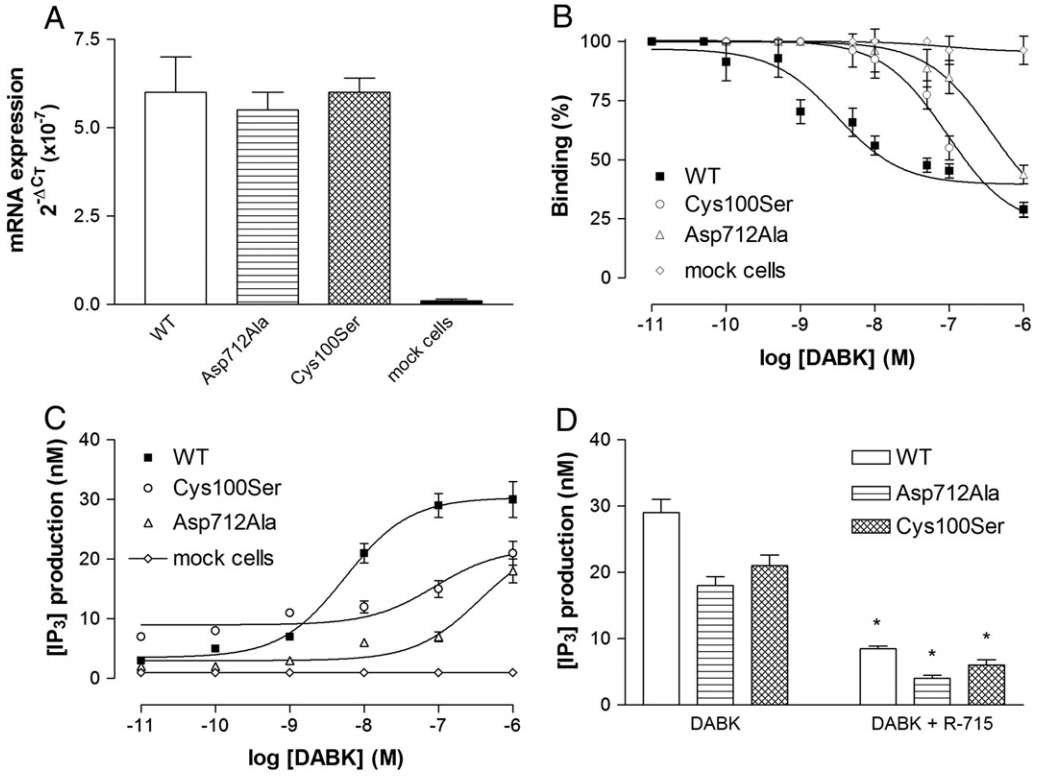

Fig. 3. Expression of wild-type and mutant kinin B_1 receptors in transfected CHO cells. A, The mRNA expression values of kinin B_1 receptor (WT), Asp712Ala, Cys100Ser mutant receptors and mock cells (expressing the empty plasmid) were quantified by real-time PCR. The values of the relative gene expression were calculated as $2^{-\Delta CT}$ parameter, which is obtained by subtracting the C_T (threshold cycle) of gene target from the C_T of internal standard. B, Competition binding profile between des-Arg^{10}[3,4-prolyl-3,4-^{3}H(N)] and increasing concentrations of the unlabeled des-Arg^9-bradykinin (DABK) in CHO cells expressing the wild-type, mock and kinin B_1 receptor mutant. Data are expressed as the percentage of maximum specific binding of the radioligand. C, IP_3 productions were obtained in response to various concentrations of DABK in CHO cells expressing the wild-type, mock and kinin B_1 receptor mutant. The DABK effect was calculated in relation to the maximal effect of the peptide. D, Effect of B_1R antagonist on the IP_3 productions induced by DABK (100 nM) in CHO cells expressing the wild-type and kinin B_1 receptor mutant. DABK induced effect was tested in the presence or absence of R-715 (1 μM), a specific antagonist of B_1R, preincubated for 30 min. Data are means ± SD of three experiments *different from WT ($P<0.05$).

Table 4
DABK and analogs' induced effect on inositol triphosphate production in wild-type and mutant kinin B_1 receptors.

Compound	Analogs	WT		Asp712Ala		Cys100Ser	
		IP_3					
		pD_2	E_{max}	pD_2	E_{max}	pD_2	E_{max}
1	DABK	8.2 ± 0.1 (3)	30 ± 0.6 (3)	6.4 ± 0.3 (3)[b]	23 ± 5.3 (3)	7.0 ± 0.3 (3)[b]	22 ± 2.7 (3)
2	A^1-DABK	6.7 ± 0.1 (3)[a]	23 ± 1.6 (3)	6.4 ± 0.2 (3)[b]	23 ± 3.7 (3)	6.9 ± 0.1 (3)[b]	20 ± 0.1 (3)
3	A^2-DABK	7.0 ± 0.1 (3)[a]	22 ± 1.4 (3)	6.6 ± 0.3 (3)[b]	19 ± 3.2 (3)	6.8 ± 0.1 (3)[b]	20 ± 0.6 (3)
4	A^3-DABK	7.3 ± 0.1 (3)[a]	23 ± 0.7 (3)	6.1 ± 0.2 (3)[b]	28 ± 5.5 (3)	6.4 ± 0.2 (3)[b]	25 ± 3 (3)
5	A^4-DABK	7.1 ± 0.1 (3)[a]	26 ± 1.2 (3)	6.2 ± 0.3 (3)[b]	24 ± 6.6 (3)	6.6 ± 0.1 (3)[b]	23 ± 1 (3)
6	A^5-DABK	8.1 ± 0.2 (3)	26 ± 1.7 (3)	6.4 ± 0.1 (3)[b]	23 ± 2.2 (3)	7.1 ± 0.1 (3)[b]	19 ± 0.5 (3)
7	A^6-DABK	8.1 ± 0.2 (3)	29 ± 1.8 (3)	6.5 ± 0.2 (3)[b]	21 ± 3.1 (3)	7.0 ± 0.1 (3)[b]	21 ± 1 (3)
8	A^7-DABK	8.0 ± 0.1 (3)	23 ± 1.25 (3)	6.5 ± 0.1 (3)[b]	21 ± 1.0 (3)	7.4 ± 0.1 (3)[b]	19 ± 0.6 (3)
9	A^8-DABK	6.8 ± 0.1 (3)[a]	19 ± 1.67 (3)	5.8 ± 1.0 (3)[b]	41 ± 54.1 (3)	6.2 ± 0.5 (3)[b]	17 ± 5 (3)
10	K^0-DABK	7.7 ± 0.2 (3)	26 ± 2.1 (3)	6.1 ± 0.7 (3)[b]	27 ± 19.4 (3)	6.6 ± 0.2 (3)[b]	23 ± 0.3 (3)
11	K^1-DABK	8.6 ± 0.1 (3)	34 ± 1.6 (3)	6.5 ± 0.3 (3)[b]	24.5 ± 5.5 (3)	7.3 ± 0.1 (3)[b]	21 ± 1 (3)
12	L^4-DABK	7.6 ± 0.1 (3)	15.5 ± 0.7 (3)	6.0 ± 0.4 (3)[b]	31 ± 14.2 (3)	6.9 ± 0.1 (3)[b]	19 ± 0.1 (3)

The IP_3 productions were obtained in response to increasing concentrations of DABK and analogs in cells expressing either the wild-type or the kinin B_1 mutant receptors. The pD_2 values (negative logarithm of the agonist concentration (M) that induces 50% of the maximal effect) were extracted from the concentration-response sigmoid logistic curves. The maximal effect (E_{max}) was calculated in relation to the maximal effect of each peptide. Data are means ± S.D. and (n) number of experiments. DABK = Arg^1-Pro^2-Pro^3-Gly^4-Phe^5-Ser^7-Pro^7-Phe^8.
[a] Different from DABK. $P<0.05$.
[b] Different of respective peptide from WT receptor. $P<0.05$.

from 2 to 8 nM (Table 3). A similar proportion of values were found for EC_{50} values related to IP_3 formation and calcium mobilization (Tables 4 and 5).

3.3. Parameters for interaction of Asp712Ala mutated B_1R and DABK analogs

Parameters for interaction of DABK and its analogs with the mutant Asp712Ala were drastically modified in relation to those observed for the wild receptor. In fact, IC_{50} values varied from 3 to 370 nM for binding affinity (Table 3), for EC_{50} values from 6 to 360 nM for IP_3 formation (Table 4) and from 4 to 192 nM for calcium mobilization to B_1R (Table 5). E_{max} values for the three parameters were not correlated to the several amino acids residues of the analogs (Tables 3–5).

Bindings of DABK analogs to the mutated receptor were shown to be weaker than those of the same analogs to wild receptor but keeping the same profile, except for the R^1 residue. The A^2-, A^4- and A^8-DABK analogs caused a range of binding affinity (IC_{50} values) varying from 400 to 900 nM and from 200 to 640 nM for A^5- and A^7-DABK analogs. The IC_{50} value for A^1-DABK analog devoid of R^1-DABK residue was 170 nM. As for wild receptor, a similar proportion of values were found for EC_{50} values for IP_3 formation and calcium mobilization (Tables 4 and 5).

3.4. Parameters for interaction of Cys100Ser mutated B_1R and DABK analogs

Absence of the second disulfide bond in Cys100Ser mutated B_1R caused a deleterious effect on the binding affinity of A^2-, A^3-, A^4- and especially of A^8-DABK (Table 3). The profile for changes was quite similar to that produced by Asp712Ala mutant receptor. However the increases in EC_{50} values were lower than those observed with wild receptor. Effects on IP_3 formation and calcium mobilization followed a same profile (Tables 4 and 5). Thus it is plausible to associate the two mutations to a same effect on the receptor leading to the modification of the extracellular site structure. A fact remaining to be explained is why the binding of F^8-DABK analog was so reduced upon receptor Cys^{650} mutation by the same rate that observed for the Asp712Ala mutant, (Table 3).

Table 5
Intracellular calcium mobilization in response to DABK and DABK analogs on wild-type and mutant kinin B_1 receptors.

Compound	Analogs	WT		Asp712Ala		Cys100Ser	
		$[Ca^{2+}]_i$					
		pD_2	E_{max}	pD_2	E_{max}	pD_2	E_{max}
1	DABK	8.3 ± 0.2 (3)	3240 ± 241 (3)	6.7 ± 0.1 (3)[b]	2307 ± 183 (3)	7.0 ± 0.3 (3)[b]	2092 ± 292 (3)
2	A^1-DABK	6.8 ± 0.6 (3)[a]	1957 ± 481 (3)	6.6 ± 0.1 (3)[b]	2087 ± 206 (3)	6.9 ± 0.1 (3)[b]	1956 ± 65 (3)
3	A^2-DABK	7.5 ± 0.2 (3)[a]	1650 ± 121 (3)	6.0 ± 0.3 (3)[b]	2342 ± 1269 (3)	6.4 ± 0.4 (3)[b]	2486 ± 630 (3)
4	A^3-DABK	7.5 ± 0.3 (3)[a]	1844 ± 202 (3)	6.1 ± 0.3 (3)[b]	2767 ± 724 (3)	6.3 ± 0.7 (3)[b]	2578 ± 1122 (3)
5	A^4-DABK	7.5 ± 0.3 (3)[a]	1615 ± 173 (3)	6.0 ± 0.3 (3)[b]	2123 ± 955 (3)	6.6 ± 0.2 (3)[b]	2120 ± 312 (3)
6	A^5-DABK	8.0 ± 0.1 (3)	2899 ± 181 (3)	6.3 ± 0.2 (3)[b]	1793 ± 417(3)	7.4 ± 0.2 (3)[b]	1977 ± 167 (3)
7	A^6-DABK	8.5 ± 0.3 (3)	3396 ± 291 (3)	6.5 ± 0.2 (3)[b]	2302 ± 359 (3)	7.1 ± 0.1 (3)[b]	1994 ± 64 (3)
8	A^7-DABK	8.2 ± 0.1 (3)	3060 ± 147 (3)	6.6 ± 0.3 (3)[b]	2320 ± 362 (3)	7.1 ± 0.1 (3)[b]	2013 ± 79 (3)
9	A^8-DABK	7.0 ± 0.2 (3)[a]	1991 ± 233 (3)	5.9 ± 0.4 (3)[b]	2393 ± 558 (3)	6.4 ± 0.5 (3)[b]	2528 ± 775 (3)
10	K^0-DABK	8.0 ± 0.4 (3)	2638 ± 338 (3)	6.4 ± 0.3 (3)[b]	2490 ± 547 (3)	7.1 ± 0.2 (3)[b]	2084 ± 179 (3)
11	K^1-DABK	8.7 ± 0.3 (3)[a]	3057 ± 266 (3)	6.3 ± 0.2 (3)[b]	2555 ± 475 (3)	7.2 ± 0.1 (3)[b]	2069 ± 121 (3)
12	L^4-DABK	6.5 ± 0.4 (3)[a]	1160 ± 218 (3)	5.9 ± 0.5 (3)[b]	2608 ± 898 (3)	6.5 ± 0.1 (3)[b]	2059 ± 168(3)

The intracellular calcium ($[Ca^{2+}]_i$) changes were obtained in response to increasing concentrations of DABK and analogs in cells expressing either the wild-type or the kinin B_1 mutant receptors. The pD_2 values (negative logarithm of the agonist concentration (M) that induces 50% of the maximal response) were extracted from the concentration-response sigmoid logistic curves. The maximal effect (E_{max}) was calculated in relation to the effect of each peptide. Data are means ± S.D. and (n) number of experiments. DABK = Arg^1-Pro^2-Pro^3-Gly^4-Phe^5-Ser^7-Pro^7-Phe^8.
[a] Different from DABK. $P<0.05$.
[b] Different of respective peptide from WT receptor. $P<0.05$.

4. Discussion

4.1. Structural requirements for DABK binding to kinin B_1 receptor

Present study shows that the residues R^1, P^2, P^3, G^4 and F^8 play major roles in DABK binding to the B_1R. Previous report on the biologic activity of these peptide analogs over the same receptor is in general agreement with these results [21]. R^1 certainly is the main binding-involved residue, at least at the N_t side of the peptide by acting through its positive charge which can be perfectly replaced by Lys (Table 3) without loss of binding affinity. In the extreme ends of DABK, other complex mechanisms than those dependent on the type of residue side-chain, ought to be considered in order to explain the effects observed.

In the C_t side, the DABK F^8 side-chain seems to be decisive for peptide binding and activity-triggering as denoted by the values in Tables 2–5 but it might also be accessory considering the importance of the special binding of the C_t carboxylate with the helix III Lys^{323} [10] and helix V Arg^{508} [11] residues at the external half of receptor 7TM central cavity. This association makes DABK the full-agonist of B_1R receptor whereas kinin B_2 receptor is able to bind BK since it contains an additional locus located one position ahead of its structure to bind the residue R^9 of this peptide.

Binding of N_t segment of DABK to kinin B_1R still seems to display a dependence on residues that are occupying positions-2, -1 and -0, preceding the positions 1–8 of the peptide itself. For instance, the presence of K^0, as in kallidins, impairs the binding and activity of rat or mouse B_1R a little but considerably affects the same properties of these receptors coming from other species as man, rabbit, cow and others. No explanation has been available yet in order to explain this difference [22].

4.2. Factors regulating DABK binding to the kinin B_1 receptor

A specific salt bridge between the DABK R^1 side-chain and B_1R Asp^{712} seems to be the basic component for a wild-type binding mode involving peptide and receptor [12]. As an indication of this condition, IC_{50} values of 3 nM or 152 nM are found for complexes between the wild-type receptor and DABK or A^1-DABK in which the bond is present or not, respectively (first and second lines of the first IC_{50} data column in Table 3). For complexes between wild-type receptor and A^2-, A^3- and A^4-DABK analogs (Table 3, first data column), the IC_{50} values are between 3 and 152 nM, thus denoting that the binding was weakened by effects due to local mutation of P^2, P^3 and G^4 to Ala. For DABK with Ala at positions 5–7, the binding was wild-like but decreased again for the A^8-DABK analog thus indicating a special binding mode for the peptide F^8 residue.

On the other side, if the specific salt bridge is eliminated upon an Asp712Ala mutation in the B_1R, other event leading to weakening of the peptide binding seems to take place. This is indicated by IC_{50} values shown in the middle IC_{50} data column (Table 3) that are found following the trend of variation of the corresponding data in the first column but at a higher level of IC_{50} values. The sole exception for this correlation was the binding of A^1-DABK analog to mutated receptor for which the IC_{50} value of 172 nM was comparable to the IC_{50} value of 152 nM observed for the binding of the same analog to wild receptor. Thus, the logical conclusion hypothesized from this finding, was that the presence of free R^1 residue in DABK analogs is responsible by a systematic weakening of the interaction of these compounds with receptor.

It is opportune at this point to analyze, how the loss of the second extracellular bond Cys^{100}–Cys^{650} might have affected the binding mode of DABK and analogs to Cys100Ser-mutated B_1 receptor (Table 3). As described, the profile of variation for effects obtained with the Asp^{712} and Cys^{100} mutations seems to be similar. However, differences between IC_{50} values obtained with analogs and mutated receptors in relation to the corresponding values with analogs and wild receptors are higher for Asp^{712} mutation than for Cys^{100} mutation.

This aspect cannot be related to the factors considered for Asp^{712}-mutated receptors since specific salt-bridge and free-peptide-Arg^1 conditions (except for A^1-DABK bindings) are equally present in complexes involving DABK and analogs, Cys^{100}-mutated and wild receptors. Thus, a distinct effect on the extracellular site produced by loss of the disulfide bond remains to be considered being it transmitted to other regions of the receptor thereby affecting the whole peptide binding. This transmission might follow a pathway formed by receptor sub-loci with specificity for binding DABK residue positions 2, 3, 4 and 8 for which mutation to Ala gave rise to receptor binding with higher IC_{50} values (Table 3).

The large effect on DABK binding to B_1R due to exchange of the peptide F^8 residue remains only partially explained. It is present in both Asp^{712}- and Cys^{100}-mutated receptors and starts as a disarrangement of the extracellular site structure at the other side of the receptor 7TM bundle. It is possible that a general binding of the DABK C_t, involving the F^8 residue and the carboxylate group to receptor locus flanked by helices III, V and VI, could work like an anchor holding the peptide inside the binding locus, probably following a bimodal mechanism of binding to be arisen along the next sections.

4.3. DABK binding site in B_1 receptor

Thus, three major connections have now been recognized in the DABK-B_1R complex: (a) a specific salt-bridge (Table 3) between peptide R^1 residue and receptor extracellular site Asp^{712}; (b) a salt-bridge between the receptor C_t carboxylate and receptor helix III Lys^{323} [10] and helix V Arg^{508} [11]; and (c) aromatic-ring interactions involving the DABK F^8 residue and aromatic residues placed in the middle of receptor helix VI (Tyr^{621}, His^{622}, Phe^{623} and Phe^{624}), [12].

The present picture allows us to point out to a very plausible condition in which the molecule of bound-agonist is shown as a U-shaped figure (Fig. 4). The first arm of this figure is linked to the receptor extracellular site via R^1-Asp^{712} bridge. The interaction of the

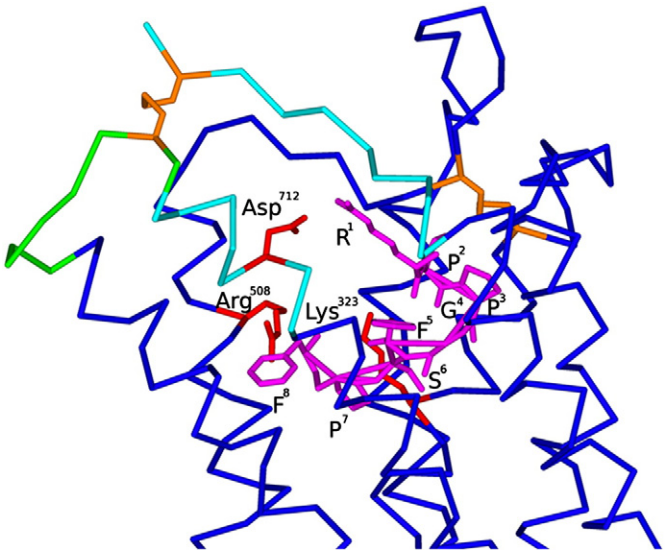

Fig. 4. Association of des-Arg^9-Bradykinin with kinin B_1 receptor. An amplified version of the structure showing the receptor the seven transmembrane-helix bundle in dark blue and the conserved Cys^{315}–Cys^{470} disulfide bond in gold. The receptor extracellular site is shown in the top of the figure consisting of N_t and EC3 segments (light blue), the Cys^{650}–Cys^{100} disulfide bond (gold) and the residue insertion (green). The peptide inserted into a postulated binding site with a horseshoe configuration is shown in magenta, the peptide C-carboxylate and receptor helix V Arg^{508} and helix III Lys^{323} and the peptide N-terminal Arg^1 side-chain and the receptor extracellular site Asp^{712}.

second arm consists of two components, the first one represented by the binding of the C_t peptide residue F^8 to a very conserved receptor aromatic-ring cluster and the second one by the binding of the peptide C_t carboxylate to the positive side-chains of helix III Lys^{323} [10] and helix V Arg^{508} [11]. The apparently non-bonded peptide F^5, S^6 and P^7 residues is distributed over the bend of the horseshoe, a condition that is consistent since these residues are not important for peptide activity (Table 2), binding (Table 3) and participation in post-activation events as IP_3 formation and calcium mobilization (Tables 4 and 5).

4.4. Concluding remarks

In short, experimental data of the current work could emphasize some remarkable points about the interaction mode of DABK to B_1R.

(1) The residues of F^5, H^6 and P^7, devoid of importance for biological activity, agonist binding and post-activation events, are in the middle of the peptide sequence.
(2) A model of B_1R built from chemokine $CXCR_4$ receptor, shows that, in order to fulfill all interactions suggested by previous mutagenesis studies, DABK has to exhibit a U-shaped configuration so that its extremes are bound to two distinct but close regions of the receptor (Fig. 4) and its middle bend is probably in a non-bonded condition.
(3) This scheme indicates that the interaction of DABK with B_1R is bimodal. The N_t extreme of the peptide binds at the extracellular site of receptor whereas the C_t extreme binds at a locus flanked by the extracellular halves of helices III, V and VI.
(4) Modifications carried out on the extracellular site of B_1R as Asp712Ala and Cys100Ser mutations, reduced the binding of DABK analogs to these mutated receptors and the activity elicited by this binding, by a process that followed the same profile previously observed with binding of DABK analogs to wild receptor. That is, for both wild and mutated receptors structural modifications were more deleterious for binding of peptide analogs when residues were changed at both extremes than at the middle of the peptide sequences. This fact would require that Asp712Ala and Cys100Ser mutations should induce equally modifications on the other side of the receptor structure, namely at the subsite for binding DABK C_t F^8 residue and C-carboxylate as widely shown in Tables 3–5. In general, the symmetrical distribution of modifications induced on B_1R structure would have a unique development: structure of receptor may be modified by residue mutations but the U-shaped configuration of DABK forming an overall complex with the receptor is kept unchanged.

Acknowledgments

This study was supported by grants from São Paulo State Research Foundation (FAPESP) and by the Brazilian National Research Council (CNPq).

References

[1] Vroling B, Sanders M, Baakman C, Borrmann A, Verhoeven S, Klomp J, Oliveira L, de Vlieg J, Vriend G. GPCRDB: information system for G protein-coupled receptors. Nucleic Acids Res 2011;39:D309–19.
[2] Palczewski K, Kumasaka T, Hori T, Behnke CA, Motoshima H, Fox BA, Trong IL, Teller DC, Okada T, Stenkamp RE, Yamamoto M, Miyano M. Crystal structure of rhodopsin: a G protein-coupled receptor. Science 2000;289:739–45.
[3] Correa SA, Pignatari GC, Ferro ES, Pacheco NA, Costa-Neto CM, Pesquero JB, Oliveira L, Paiva AC, Shimuta SI. Role of the Cys18–Cys274 disulfide bond and of the third extracellular loop in the constitutive activation and internalization of angiotensin II type 1 receptor. Regul Pept 2006;134:132–40.
[4] Hjorth SA, Schambye HT, Greenlee WJ, Schwartz TW. Identification of peptide binding residues in the extracellular domains of the AT1 receptor. J Biol Chem 1994;269:30953–9.
[5] Costa-Neto CM, Miyakawa AA, Oliveira L, Hjorth SA, Schwartz TW, Paiva AC. Mutational analysis of the interaction of the N- and C-terminal ends of angiotensin II with the rat AT(1A) receptor. Br J Pharmacol 2000;130:1263–8.
[6] Noda K, Saad Y, Karnik SS. Interaction of Phe8 of angiotensin II with Lys199 and His256 of AT1 receptor in agonist activation. J Biol Chem 1995;270:28511–4.
[7] Feng YH, Noda K, Saad Y, Liu XP, Husain A, Karnik SS. The docking of Arg2 of angiotensin II with Asp281 of AT1 receptor is essential for full agonism. J Biol Chem 1995;270:12846–50.
[8] Noda K, Saad Y, Kinoshita A, Boyle TP, Graham RM, Husain A, Karnik SS. Tetrazole and carboxylate groups of angiotensin receptor antagonists bind to the same subsite by different mechanisms. J Biol Chem 1995;270:2284–9.
[9] Oliveira L, Costa-Neto CM, Nakaie CR, Schreier S, Shimuta SI, Paiva AC. The angiotensin II AT1 receptor structure–activity correlations in the light of rhodopsin structure. Physiol Rev 2007;87:565–92.
[10] Leeb T, Mathis SA, Leeb-Lundberg LM. The sixth transmembrane domains of the human B1 and B2 bradykinin receptors are structurally compatible and involved in discriminating between subtype-selective agonists. J Biol Chem 1997;272:311–7.
[11] Santos EL, de Picoli Souza K, Cibrian-Uhalte E, Oliveira SM, Bader M, Costa-Neto CM, Oliveira L, Pesquero JB. Essential role of TM V and VI for binding the C-terminal sequences of Des-Arg-kinins. Int Immunopharmacol 2008;8:282–8.
[12] Ha SN, Hey PJ, Ransom RW, Bock MG, Su DS, Murphy KL, Chang R, Chen TB, Pettibone D, Hess JF. Identification of the critical residues of bradykinin receptor B1 for interaction with the kinins guided by site-directed mutagenesis and molecular modeling. Biochemistry 2006;45:14355–61.
[13] Barany G, Marrifield RB. The peptides: analysis, synthesis and biology. New York: Academic Press; 1980.
[14] Nakaie CR, Oliveira E, Vicente EF, Jubilut GN, Souza SE, Marchetto R, Cilli EM. Solid-phase peptide synthesis in highly loaded conditions. Bioorg Chem 2011;39:101–9.
[15] Nsa Allogho S, Gobeil F, Pheng LH, Nguyen-Le XK, Neugebauer W, Regoli D. Antagonists for kinin B1 and B2 receptors in the mouse. Can J Physiol Pharmacol 1997;75:558–62.
[16] Allogho SN, Gobeil F, Pheng LH, Nguyen-Le XK, Neugebauer W, Regoli D. Kinin B1 and B2 receptors in the mouse. Can J Physiol Pharmacol 1995;73:1759–64.
[17] Abe KC, Mori MA, Pesquero JB. Leptin deficiency leads to the regulation of kinin receptors expression in mice. Regul Pept 2007;138:56–8.
[18] Livak KJ, Schmittgen TD. Analysis of relative gene expression data using real-time quantitative PCR and the 2(−delta delta C(T)) method. Methods 2001;25:402–8.
[19] Vriend G. WHAT IF: a molecular modeling and drug design program. J Mol Graph 1990;8:52–6.
[20] Wu B, Chien EY, Mol CD, Fenalti G, Liu W, Katritch V, Abagyan R, Brooun A, Wells P, Bi FC, Hamel DJ, Kuhn P, Handel TM, Cherezov V, Stevens RC. Structures of the CXCR4 chemokine GPCR with small-molecule and cyclic peptide antagonists. Science 2010;330:1066–71.
[21] Marceau F, Regoli D. Bradykinin receptor ligands: therapeutic perspectives. Nat Rev Drug Discov 2004;3:845–52.
[22] Leeb-Lundberg LM, Marceau F, Muller-Esterl W, Pettibone DJ, Zuraw BL. International union of pharmacology. XLV. Classification of the kinin receptor family: from molecular mechanisms to pathophysiological consequences. Pharmacol Rev 2005;57:27–77.